Proceedings of the 29th Annual International
Conference of the IEEE EMBS
Cité Internationale, Lyon, France
August 23-26, 2007.

Balloon folding affects the symmetry of stent deployment: experimental and computational evidence

Andrew J Narracott, Patricia V Lawford, Julian PG Gunn, D Rodney Hose

Abstract— **The level of restenosis following coronary artery stenting may be related to the deployed stent geometry. This study investigated the influence of two balloon folding patterns ('C' and 'S' shaped) on stent deployment. *In vitro* stent expansion showed 'S' shape folding produced more uniform expansion than 'C' shape folding. A numerical contact model (NCM) was developed to study the detail of load transfer between balloon and stent. Finite element analysis of the Palmaz-Schatz 204C stent provided a composite non-linear material model for the NCM. Agreement between the predicted final stent geometry and experimental results was strongly dependent on the frictional coefficient between the stent and balloon. We conclude that non-uniform contact may contribute to the asymmetry of deployed stents reported clinically.**

I. Introduction

It is suggested that the degree of restenosis in stented coronary arteries is related to the symmetry of stent deployment with greater intimal thickening associated with uneven deployment [1-3]. Whilst stents are known to deploy asymmetrically in the presence of calcified lesions [4,5], the effects of stent design, balloon folding and lesion characteristics on deployment symmetry are unknown.

This study examines the effect of balloon folding on deployment symmetry. A computational numerical contact model (NCM) is developed and model results are compared with *in vitro* deployment. We suggest that the pattern of balloon folding plays an important role in determining the final stent geometry. This has implications for the variation of forces during deployment and, in the clinical situation, the forces transmitted by the stent and balloon to the surrounding tissue. This aspect of variability during stent deployment has been identified by other authors [6,7] but there has been no attempt to quantify these effects.

II. Methods

A. Experimental measurement of stent expansion

The Palmaz-Schatz 204C stent was chosen as this has a well-defined cellular geometry that can be represented with a small number of measurements. *In vitro* deployment of the stent [8,9] allowed direct comparison with the model results. The stent was deployed with the balloon folded into either a 'C' or an 'S' shaped folding pattern as shown in Fig. 1a. These folding patterns are expected to produce one and two internal 'lobes' respectively during deployment, as illustrated in Fig. 1b. The balloon was inflated to its rated burst pressure (12 atm, 1.26MPa) using a Merit Medical Basix25 inflation device.

B. Development of a NCM of stent/balloon interaction during stent deployment

1) Assumptions

The assumptions made in the development of the NCM are as follows:

- the system can be represented by a 2D plane strain analysis. Stents are designed to undergo minimal length changes. In practice 'dog-boning' (when the ends of the stent expand first) can occur. This effect cannot be captured by the proposed methodology.
- the balloon is inextensible. The balloons are described as 'non-compliant' and, in practice, strain in the balloon is likely to be small until the stent is fully deployed.
- the balloon remains in contact with the stent, except over discrete 'gaps' (of length g) at the lobes. Sensitivity of the model results to this parameter are discussed later.
- at the 'gaps' all of the circumferential membrane load is carried by the stent. Away from these locations the load in the stent reduces based on effective frictional contact between the balloon and the stent.
- the effective coefficient of friction between the stent and the balloon is constant during deployment.
- an effective constitutive equation for the stent can be determined from a separate 3D finite element analysis.
- circumferential bending stresses in both the balloon [10] and stent are negligible, so equilibrium of the system can be described in terms of the membrane equations. The bending of the struts of the stent during deployment is included in the effective constitutive relationship.

The geometry of the model is illustrated in Fig. 2. Appropriate symmetry conditions were applied to reduce the size of the domain, giving a 180° segment for the C-fold and a 90° segment for the S-fold pattern.

Manuscript received June 22nd, 2007. This work was supported by the EPSRC and Medtronic/AVE, Galway.

AJ Narracott is with the Academic Unit of Medical Physics, University of Sheffield, I floor, Royal Hallamshire Hospital, Glossop Road, Sheffield, S10 2JF, UK (phone: +44 114 2712180; fax: +44 114 2713403; e-mail: a.j.narracott@sheffield.ac.uk).

PV Lawford and DR Hose are with the Academic Unit of Medical Physics, University of Sheffield, UK.

JPG Gunn is with the Cardiovascular Research Unit, Section of Cardiovascular Sciences, University of Sheffield, UK.

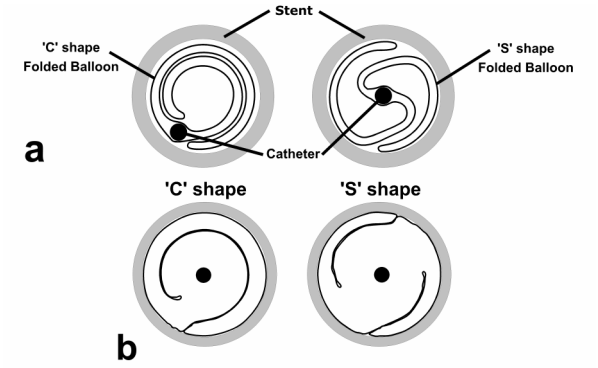

Figure 1: Balloon lobe geometry a) Balloon geometry after folding and stent placement b) Anticipated balloon geometry during inflation process illustrating development of 'C' shape single lobe and 'S' shape double lobe.

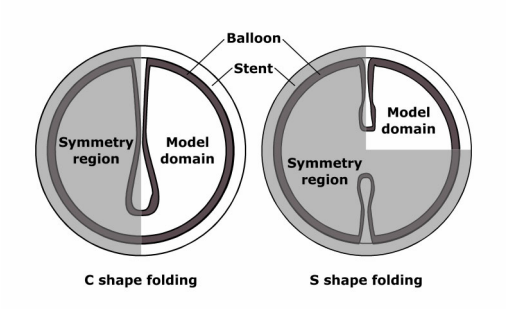

Figure 2: Geometry of the Numerical Contact Model (NCM) showing extent of the model domain for both the 'C' and 'S' shape balloon folding .

2) Equilibrium equations

In the following, N is the force per unit axial length of the model and R is the mean radius of the stent (the internal radius plus half the stent thickness).

For equilibrium of the balloon in the radial direction:

$$P_c = P_b - \frac{N_{\theta b}}{R} \tag{1}$$

where P_c is the contact pressure between balloon and stent, P_b is the balloon pressure, $N_{\theta b}$ is the circumferential force per unit axial length in the balloon. Equilibrium of the balloon in the circumferential direction gives the force carried by the balloon, assuming that the stent and balloon are at the point of sliding at all locations:

$$\frac{dN_{\theta b}}{dx} = -\tau = \mu P_c = \mu\left(P_b - \frac{N_{\theta b}}{R}\right) \tag{2}$$

where x is the circumferential distance, τ is the shear stress on the stent and μ is the coefficient of friction between stent and balloon. The solution to equation 2 is given by:

$$N_{\theta b} = P_b R\left(1 - e^{-\mu x / R}\right) \tag{3}$$

The force carried by the stent is then determined by considering equilibrium of the stent in the radial direction:

$$N_{\theta s} = P_c R = P_b R - N_{\theta b} \text{ and } N_{\theta s} = P_b R\left(e^{-\mu x / R}\right) \tag{4}$$

where $N_{\theta s}$ is the force per unit axial length carried by the stent.

3) Compatibility relation

From equation 4, the force in the stent at a particular balloon pressure depends on the value of pressure, P_b, the coefficient of friction, μ, and the mean radius, R, which itself varies with pressure. As compatibility is required between the circumferential strain and applied force, the value of R is determined with knowledge of the nonlinear constitutive relationship for the stent which is given by a separate finite element analysis described in section IIC.

The nonlinear equilibrium and compatibility equations were solved simultaneously using Matlab (Mathworks) by discretizing the stent geometry circumferentially into M elements, as follows:

4) Discretized solution

For a given value of mean stent radius, R, deformed, L, and undeformed, L_0, element lengths are defined as follows:

$$L = \frac{S_C R}{M} \text{ and } L_0 = \frac{S_C R_0}{M} \tag{5}$$

with $S_c = \pi$ (C shape) and $\pi/2$ (S shape) folding

For each of the M elements the force is assumed to be constant throughout each element and is given by:

$$N_{\theta s}^m = P_{trial} R \text{ if } x_m < g/2 \tag{6}$$

$$N_{\theta s}^m = P_{trial} R\left\{e^{[-\mu(x_m - g/2)/R]}\right\} \text{ if } x_m > g/2 \tag{7}$$

where $N_{\theta s}^m$ is the force per unit axial length in the mth element, P_{trial} is a trial value of the balloon pressure (initially zero), g is the contact gap and x_m is the circumferential distance of the centre of the mth element:

$$x_m = (m-1)L + L/2 \tag{8}$$

$N_{\theta s}^m$ is calculated for all elements based on the trial pressure value. The strain in each element, ε^m, is determined from the relationship with $N_{\theta s}^m$ given by the finite element analysis. A mean radius, R_{calc}, is calculated consistent with the strains due to the trial pressure value:

$$R_{calc} = \frac{1}{S_C}\left(L_0 M + L_0 \sum_1^M \varepsilon^m\right) \tag{9}$$

The value $R_{err} = R - R_{calc}$ is used as measure of convergence. The value of P_{trial} is increased until R_{err} is less than 0.1% of the R value.

C. Constitutive relationship for the stent

1) ANSYS model geometry and boundary conditions

The constitutive relationship for the stent was obtained by constructing a 3d finite element model of the stent within ANSYS 5.6 (Ansys Inc, Canonsburg, USA) using 20 node SOLID186 elements to define the stent geometry. Symmetry was exploited to model a 30° segment of the stent in the circumferential direction, of axial length L_z. The full stent geometry and symmetry section are shown in Fig. 3.

Symmetry conditions were imposed in cylindrical coordinates (r, θ, z): fixing z degrees of freedom at z = 0, fixing θ degrees of freedom at θ = 0 and θ = π/6, coupling z degrees of freedom at $z = L_z$.

Measurements of strut geometry were obtained from images of the stent during experimental testing [8,9]. Material properties were defined using data provided for stainless steel SS316L by Medtronic/AVE. Values of true stress and strain were used to provide coefficients for the ANSYS non-linear isotropic hardening (NLISO) material model. A uniform pressure was applied to the interior of the stent and this value was varied until the fully deployed stent diameter was achieved.

2) Calculation of constitutive relationship

At each increment of applied pressure the following parameters were retrieved from the ANSYS analysis: radial displacement (of the nodes on the inner surface of the stent at θ = π/6), u_r, axial displacement (of the nodes at $z = L_z$), u_z, applied stent pressure, P_s. The constitutive relationship for the stent was then calculated as follows:

$$\varepsilon = u_r / R_0 \tag{10}$$

where ε is the stent strain and R_0 is the initial internal radius of the stent. The force per unit axial length carried by the stent, $N_{\theta s}$, is given by:

$$N_{\theta s} = \frac{6 P_S A_S}{\pi L_Z} \quad \text{with } L_z = L_{z0} + u_z \tag{11}$$

where A_s is the area of the stent over which the pressure is applied, L_z is the deformed axial length of the stent, L_{z0} is the initial axial length of the stent and u_z is the axial displacement of the stent section.

ε is the engineering strain, equal to the ratio of change in radius (u_r) to initial radius (R_0). This measure of strain is consistent with the NCM where the deformed element length is related directly to the undeformed length.

The constitutive relationship derived from the ANSYS analysis is illustrated in Fig. 4. During the analysis a 150% change in stent radius resulted in only a 5% change in axial length, confirming that out of plane strains are small. Where the force exceeded the values in Fig. 5 the strain was obtained by linear extrapolation of the constitutive curve.

III. Results

A. Comparison of numerical and experimental results for Pressure v Radius

The NCM was used to predict the pressure/radius relationship using both 'S' and 'C' shape folding patterns. These results are compared with the pressure/radius relationship determined during experimental tests [8] in Fig. 5a. Four stents were deployed (two with 'C' and, two with 'S' shape folding), the pressure/radius response of the second 'S' shape deployment is unavailable due to a malfunction of the data-logging system. The results of the NCM presented here are for a model consisting of 100 elements with a frictional coefficient of 0.15 and a contact gap, g, of 0.468mm (10% of the initial stent circumference). For both the NCM and the experimental results the mean radius of the stent was used (internal stent radius plus half stent thickness).

B. Comparison of numerical and experimental results for strain distribution

The final 'inter-strut distance' (ISD) between the center of the six, initially equally spaced, bridge sections of the PS204C struts (see Fig. 3) was measured experimentally, as described previously [9]. The ISD was then used to calculate the experimental strain distribution during stent expansion as follows:

$$\varepsilon_{\exp} = \left(ISD_f - ISD_i\right) / ISD_i \tag{12}$$

where ε_{exp} is the experimental strain, ISD_f is the final inter-strut distance and ISD_i is the initial inter-strut distance of the undeployed stent.

The NCM results were used to produce comparative measures of strain by calculating the mean strains in the following groups of elements:

S fold	$\varepsilon_1, \varepsilon_4 = \frac{3}{M}\sum_{1}^{M/3}\varepsilon_m \quad \varepsilon_2, \varepsilon_3, \varepsilon_5 = \frac{3}{2M}\sum_{M/3+1}^{M}\varepsilon_m$
C fold	$\varepsilon_1 = \frac{6}{M}\sum_{1}^{M/6}\varepsilon_m \quad \varepsilon_2, \varepsilon_6 = \frac{3}{M}\sum_{M/6+1}^{M/2}\varepsilon_m$ $\varepsilon_3, \varepsilon_5 = \frac{3}{M}\sum_{M/2+1}^{5M/6}\varepsilon_m \quad \varepsilon_4 = \frac{6}{M}\sum_{5M/6}^{M}\varepsilon_m$

where ε_n is the average strain in group n, M is the total number of elements in the model and ε_m is the strain in the mth element.

The final strain distributions predicted by the NCM (contact gap, g = 0.468mm, M = 100) for several values of frictional coefficient, μ, are shown in Fig. 5b and 5c along with the experimental results for deployment of four stents (two with 'C' shape and two with 'S' shape folding). Error bars for experimental measurements represent the estimated error (±0.05mm) of the experimental measurement technique [9]. The strain is plotted relative to the circumferential index around the stent, with the first index repeated to illustrate the symmetry of the expansion.

C. Sensitivity of the NCM results to model parameters

A sensitivity study was undertaken to determine the relative influence of the frictional coefficient, μ, and contact gap, g, on both the strain distribution (maximum inter-strut strain ε_{max} and standard deviation of inter-strut strain σ_{strain}) and pressure at the fully deployed radius (P_f). The variation of results with the number of model elements, M, was also assessed. These results are given in Table 1, along with the experimental values of these variables, where appropriate.

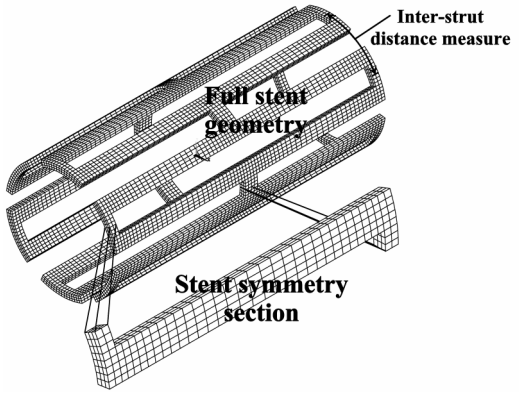

Figure 3: Finite element stent model showing the full stent geometry along with the symmetry section and the inter-strut distance measure.

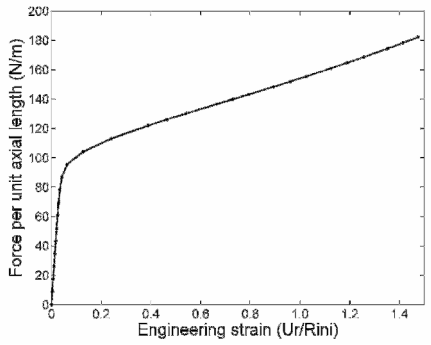

Figure 4: Constitutive relationship derived from the ANSYS analysis relating the circumferential force/unit axial length, $N_{\theta s}$, in the stent to the engineering strain, ε, based on the change in radius.

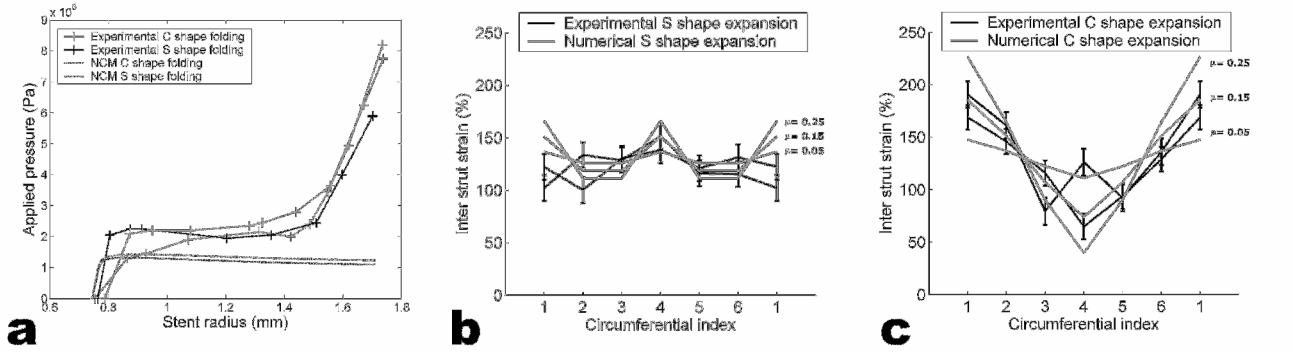

Figure 5: Comparison of experimental and numerical contact model results a) pressure/radius relationship. b) strut distributions for 'S' shape folding c) strut distributions for 'C' shape folding. Strut distributions are shown for three values of frictional coefficient, μ. The circumferential index provides the relative position of the struts around the circumference of the stent.

TABLE 1
VARIATION IN SOLUTION VALUES WITH CHANGE IN MODEL INPUT PARAMETERS.
RESULTS ARE FROM THE NCM UNLESS INDICATED (EXP = EXPERIMENTAL RESULTS).

Fold	μ x100	g (mm)	M	P_f (Pa)	ε_{max} (%)	σ_{strain}	Fold	μ x100	g (mm)	M	P_f (Pa)	ε_{max} (%)	σ_{strain}
S	5	0.47	100	1.03e5	136	5	C	5	0.47	100	1.07e5	147	13
S	15	0.47	100	1.10e5	151	17	C	15	0.47	100	1.23e5	185	42
S	25	0.47	100	1.17e5	166	29	C	25	0.47	100	1.41e5	226	72
S	15	0	100	1.12e5	151	17	C	15	0	100	1.26e5	186	43
S	15	0.94	100	1.08e5	149	16	C	15	0.94	100	1.21e5	183	41
S	15	0.47	50	1.10e5	150	17	C	15	0.47	50	1.23e5	186	43
S	15	0.47	200	1.10e5	151	17	C	15	0.47	200	1.23e5	186	43
Exp S1	-	-	-	-	138	12	Exp C1	-	-	-	~2e5	190	44
Exp S2	-	-	-	~2e5	151	17	Exp C2	-	-	-	~2e5	170	39

IV. DISCUSSION

From Fig. 5b and 5c it is clear that the two folding patterns result in distinct strain distributions. It should be noted that, given an initially uniform distribution of ISD, a symmetrically deployed stent would produce a horizontal line in these plots, the level of deviation from this condition represents the degree of asymmetry in deployment. 'C' shape folding produced a characteristically sinusoidal distribution of strain, with a clear preference for deployment of one side of the stent. 'S' shape folding produced more even expansion, with some areas of localized strain. We suggest the regions of highest strain seen experimentally correspond to the positions of the lobes of the balloon.

The NCM results were shown to be relatively insensitive to variation in the model parameters with the exception of the frictional coefficient between the stent and the balloon, μ.

The distribution of strain within the deployed stent predicted by the NCM was in good agreement with experimental strain distributions for μ = 0.15. The difficulty of predicting frictional coefficients for complex systems is acknowledged but a value of 0.15 is within the range 0.12 – 0.24 for un-lubricated contact of a non-metal (balloon) with an unlike material (stent) [11]. Direct comparison of μ in the NCM with such values may be inappropriate as the frictional coefficient in the NCM represents the friction between the two materials and any

quilting of the balloon between the stent struts.

The pressure-radius response of the NCM exhibits overall characteristics in agreement with the experimental results in Fig 5a. The sharp increase in experimental pressure at the end of the expansion arises as the balloon reaches its fully inflated state, which is not included in the model. The NCM predicted deployment at pressures approximately 40% lower than experimentally observed. This disagreement is unlikely to be due to end effects which are likely to reduce the pressure required for deployment. The slope of the pressure/radius response predicted by the model becomes negative as the stent expands. This is not observed experimentally as a continual increase in pressure is required to deploy the stent fully. The NCM cannot reproduce all the complex features of stent and balloon interaction during deployment. This would require a model of the stent and balloon including 3d geometry, non-linear material properties and the variation of these during the expansion process. The disagreement between the pressure results may be due to either more complex load transfer or experimental error in the recorded pressure.

Despite such limitations, the NCM allows both a change in the pressure loading as a function of radius, due to the non-linear relationship between the balloon area and the stent area, and a discontinuous transfer of load between the balloon and the stent, due to the definition of contact and non-contact areas within the NCM. This model may be valuable for a rapid assessment of a particular folding pattern and although study of the interaction of balloon folding and arterial inhomogeneity is beyond the scope of this study, it is suggested that the NCM has merit for this application.

In relation to previous studies of stent expansion, observations of uniform deployed stent geometry [12] are supported by these results under certain balloon folding conditions. However, the assumption that the balloon acts on the stent as a uniform pressure [12-15] is not justified for all configurations of balloon folding. Furthermore, the small effects seen for certain folding patterns *in vitro* may be exaggerated during *in vivo* expansion, particularly in vessels with inhomogeneous material properties.

V. Conclusions

Variation in balloon folding leads to *in vitro* asymmetry of deployment of the Palmaz-Schatz 204C stent. Examination of load transfer was undertaken using a numerical contact model. Several features of stent expansion observed experimentally were confirmed by the NCM:

- More uniform deployment was observed using an 'S' shape (dual lobe) folding pattern than a 'C' shape (single lobe) folding pattern
- Areas of focal deployment occur at points of reduced contact between the balloon and stent
- The difference in pressure-radius response between the two modes of deployment is small
- The variation in strain occurs at an early stage during the deployment.

It is concluded that the uniformity of *in vitro* stent deployment increases with the number of 'lobes' present in the balloon folding. Each 'lobe' results in an area of reduced contact and an associated discontinuity of force transfer.

Although the use of 'C' shaped folding represents an extreme case compared with the multi-lobe folding currently in use in many deployment systems, it allows the effects of non-uniform load transfer between the balloon and the stent to be quantified experimentally. The smaller magnitude effects arising from multi-lobe folding are not expected to result in significant asymmetry of deployment *in vitro* but could combine with the non-uniform properties of diseased vessels to result in asymmetry *in vivo*. Therefore, we recommend that balloon folding effects be included in the study of stent/vessel interaction.

Acknowledgment

The authors thank Medtronic/AVE who provided material property data for SS316L, Rutherford Appleton Labs, UK and Medical Workshop, Royal Hallamshire Hospital, Sheffield, UK for development of the experimental system.

References

[1] Garasic JM, Edelman ER, Squire JC, Seifert P, Williams MS, Rogers C. Circ .101; 812-8, 2000.

[2] Rogers C, Edelmann ER. Circ. 91; 2995-3001, 1995.

[3] Schulz C, Herrmann RA, Beilharz C, Pasquantonio J, Alt E. Heart 83; 462-7, 2000.

[4] Albrecht D, Kaspers S, Fussl R, Hopp HW, Sechtem U. Cath & Cardiovasc Diag. 38; 229-35, 1996.

[5] Henneke KH, Regar E, Konig A, Werner F, Klauss V, Metz J, Theisen K, Mudra H. Am Heart J.. 137; 93-9, 1999.

[6] Lally C, Dolan F, Prendergast PJ. J Biomech 38; 1574-81, 2005.

[7] Migliavacca F, Petrini L, Montanari V, Quagliana I, Auricchio F, Dubini G. Med Eng and Phys 27;13-18, 2005.

[8] Narracott AJ. "Balloon folding affects the symmetry of stent expansion: experimental and computational evidence." PhD Thesis, University of Sheffield, Sheffield, UK, 2002.

[9] Narracott AJ, Hose DR, Lawford PV, Gunn J. Med Eng & Tech 27 59-70, 2003.

[10] Rogers C, Tseng DY, Squire JC, Edelman ER. Circulation Research 84: 378-383, 1999

[11] Rabinowicz E (1995) Friction and wear of materials. 2nd Ed, John Wiley & Sons, Inc, New York. Ed.Roark RJ, Young WC (1975)

[12] Dumoulin C, Cochelin B. J Biomech. 33;1461-70, 2000.

[13] Etave F, Finet G, Boivin M, Boyer J-C, Rioufol G, Thollet G. J Biomech 34; 1065-1075, 2001.

[14] Gu L, Santra S, Mericle RA, Kumar AV. J Biomech 38; 1221-7, 2005.

[15] Migliavacca F, Petrini L, Colombo M, Aurricchio F, Pietrabissa R. J. Biomech 35;803-11, 2002.